Structure of Grafted Polymeric Brushes in Solvents of Varying Quality: A Molecular Dynamics Study

Gary S. Grest*,† and Michael Murat‡

Corporate Research Science Laboratories, Exxon Research and Engineering Company, Annandale, New Jersey 08801, and Department of Physics and Applied Mathematics, Soreq Nuclear Research Center, Yavne 70600, Israel

Received December 21, 1992; Revised Manuscript Received March 20, 1993

ABSTRACT: A molecular dynamics simulation of polymeric brushes in solvents of varying quality is presented. The resulting equilibrium structures are compared with those predicted by self-consistent field (SCF) analysis. The scaling of the brush height is found to agree with the SCF predictions at temperatures $T > T_\Theta$, where T_Θ is the Θ temperature of the solvent. The agreement at $T < T_\Theta$ is poor, probably resulting from the separation of the brush into monomer-rich and monomer-poor phases. This phase separation disappears with increasing grafting density and chain length. Good agreement is found with the SCF predictions for the density profile of the monomers and of the free ends of the chains and for the structure factor under good solvent conditions. The agreement of these properties with the SCF predictions at and below T_Θ is not as good. Even the scaling behavior of the profiles with respect to the chain length and the grafting density is found to be inconsistent with the SCF analysis. The effect of a small attractive surface interaction on the structure of the brush is also studied.

I. Introduction

Polymeric brushes, formed by attaching (grafting) one end of a polymer onto a surface, are of both practical and theoretical interest.[1] These brushes have applications in colloidal stabilization through the utilization of the excluded volume interactions between the polymeric chains. Theoretical interest in these systems arises, since the confinement of the polymeric chains leads to configurations qualitatively different from those of free chains. During the last several years, properties of brushes under good solvent and melt conditions have been studied in detail. Following the early works of Alexander[2] and de Gennes,[3] who used a scaling approach, there have been a number of theoretical and experimental studies of the brushes. Self-consistent field (SCF) calculations, both numeric[4-9] as well as analytic[1,10,11] have been widely used. Both the scaling and SCF approaches predict that, under good solvent conditions, the brush height h scales with the chain length N and the grafting density ρ_a as $h \propto N\rho_a^{1/3}$. Furthermore, the SCF analysis predicted a parabolic decay of the monomer density from a maximum at the grafting surface to zero at h in the limit of long chains and strong overlap when binary interactions are dominant. However, at high surface coverage, where high-order interactions are relevant, the density profile is expected to be flatter than a parabola.[12,13] Computer simulations of these systems, using both molecular dynamics (MD)[14] and Monte Carlo (MC),[5,15-18] confirmed these predictions, and gave further details of the structure of the brushes. A mean field approximation in which one considers the central chain in a mean field of attractive and repulsive interactions with the molecules in the environment has recently been developed by Carignano and Szleifer.[19] Their results are in very good agreement with both lattice and off-lattice simulations. In addition both theory[20-23] and simulation[24] have been extended to curved grafting surfaces.

Experimental studies of the brushes have mostly concentrated on the force between two plates with polymers end grafted onto them.[25-28] These experiments give a direct measure of the brush height but not of the density profile. These results have been compared in detail with the predictions of the scaling and SCF analysis.[29] It was found that while both theoretical approaches describe equally well the force profile the SCF analysis[29] had fewer free parameters. A detailed MD study[30] of the compressional force between two surfaces baring end-grafted polymers not only agreed with measurements of ref 25 but also gave additional information like the monomer density and amount of interpenetration. A mapping of these simulation results to data on end-functionalized polymers can be found in the Appendix. Several experimental studies of the local structure of the brushes using small-angle neutron scattering[31-34] and neutron reflectivity[35] have found that the resulting structure factor was consistent with a parabolic density profile with a small exponential tail. It thus seems that a SCF analysis which includes only binary interactions describes rather well the structure of the polymeric brushes under good solvent conditions.

Recently the structure of brushes in solvents of different quality has been the subject of several theoretical,[7,12,36-40] simulation,[41,42] and experimental[32,43,44] studies. Zhulina *et al.*[38] performed a detailed analytic SCF analysis of polymeric brushes in the vicinity of the Θ temperature, T_Θ. They obtained explicit results for the brush height, the density profile, and the density of the free ends of the chains. Lai and Binder[41] carried out a detailed MC simulation of these systems using the bond-fluctuation model, with chains of length $N \leq 50$. They confirmed the predictions of ref 38 with respect to the variation of the brush height with N, ρ_a, and T, but found that the density profile of the monomers and of the free ends showed considerable deviation at $T \simeq T_\Theta$ from the prediction of Zhulina *et al.*[38] They also observed that below T_Θ the system phase separated into monomer-rich and monomer-poor regions. This phase separation has recently been explained within the random phase approximation by Yeung *et al.*,[40] who find that, for fixed chain length and coverage, the grafted layer is unstable to tangential fluctuations in a sufficiently poor solvent. When the mean field solutions become unstable, they find that the end-grafted polymers clump together to form a "dimpled" surface in agreement with our results as well as those by Lai and Binder.[41] See Note Added in Proof.

† Exxon Research and Engineering Co.
‡ Soreq Nuclear Research Center.

0024-9297/93/2226-3108$04.00/0

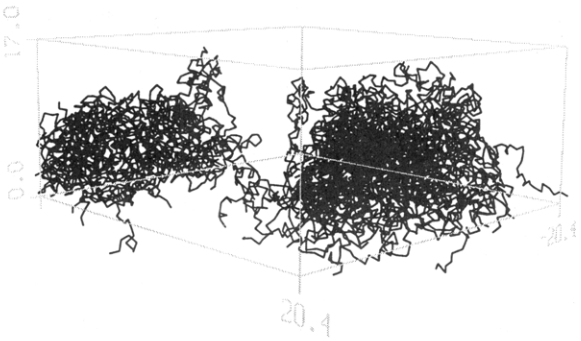

Figure 1. Typical configuration of polymer brush far below T_θ ($T = 2.0$) for 50 polymer chains of length $N = 100$ end grafted at a coverage of $\rho_a = 0.03$. Each polymer is grafted at one end randomly onto the lower surface $z = 0$. Periodic boundary conditions are used in the horizontal plane.

In this work, we perform a MD study of brushes at various temperatures, using chains of length up to $N = 200$. The simulations were performed at constant surface area. In addition to the brush height and the density profiles, we also determined the static structure factor, as is done experimentally. While the results for the good solvent case exhibit good agreement with the SCF predictions, we find increasingly worse agreement as T decreases. In some cases, we also find results differing qualitatively from those obtained in the MC simulations. We attribute these discrepancies to the wider range of N and ρ_a covered in the present work. We also find the phenomenon of "phase separation" below T_θ (see Figure 1) as observed by Lai and Binder.[41] However, we find that this effect disappears as the grafting density and the chain length increase.

In the next section, we describe the simulation method. Section III describes the results for such average quantities as the brush height and radius of gyration. In section IV, we discuss the structure of the brush in more detail for the good, θ, and bad solvent regimes. These are compared to the predictions of the SCF analysis. The effect of a small attractive interaction between the grafting surface and the monomers on the structure of the brush is discussed in section V. A short summary is presented in section VI.

II. Model and Method

The equilibrium structure of the brushes in a solvent was obtained using a molecular dynamics method in which each monomer is coupled to a heat bath. The equation of motion for monomer i (of mass m) is given by

$$m\frac{d^2\vec{r}_i}{dt^2} = -\vec{\nabla}\cdot\vec{U}_i - m\Gamma\frac{d\vec{r}_i}{dt} + \vec{W}_i(t) \tag{1}$$

where Γ is the friction coefficient that couples the monomers to the heat bath. The random part of the monomer–heat bath coupling is given by a white-noise term $\vec{W}_i(t)$, which satisfies

$$\langle \vec{W}_i(t)\cdot\vec{W}_j(t')\rangle = 6k_BTm\Gamma\delta_{ij}\delta(t-t') \tag{2}$$

Here k_B is the Boltzmann constant and T is the temperature. The potential U_i is composed of three terms: $U_i = U^0 + U^{ch} + U^w$. U^0 is a Lennard-Jones (LJ) potential:

$$U^0(r) = \begin{cases} 4\epsilon\left[\left(\frac{\sigma}{r}\right)^{12} - \left(\frac{\sigma}{r}\right)^{6} - \left(\frac{\sigma}{r_c}\right)^{12} + \left(\frac{\sigma}{r_c}\right)^{6}\right] & r \le r_c \\ 0 & r > r_c \end{cases} \tag{3}$$

In our previous studies of the brushes,[14,24,30] we had taken $r_c = 2^{1/6}\sigma$, such that the potential is purely repulsive. This is an efficient method for studying good solvent conditions. Since the potential is close to that of a hard sphere, we refer to this case as athermal for convenience. To introduce the effect of solvent quality, we extended the range of the interaction to $r_c = 2.5\sigma$. Thus, by changing T, we could vary the relative importance of the monomer–monomer attraction and change the effective quality of the solvent without explicitly introducing solvent particles.

While U^0 acts between all pairs of monomers, U^{ch} is an attractive potential binding the monomers along a chain. The form of this potential is taken as

$$U^{ch}(r) = \begin{cases} -0.5kR_0^2\ln[1-(r/R_0)^2] & r \le R_0 \\ \infty & r > R_0 \end{cases} \tag{4}$$

with $k = (T/1.2)30\epsilon/\sigma^2$ and $R_0 = 1.5\sigma$. This choice of parameters, including the temperature dependence of k, ensures that the average bond length is essentially independent of T and takes on a value of about 0.97σ.

For the wall–monomer interaction, we used two forms for the potential. The first was a purely repulsive interaction between the monomers and the grafting surface (wall) represented by

$$U^{rw} = \epsilon(\sigma/z)^{12} + Az + B \tag{5}$$

where z is the vertical distance from the grafting surface. A and B are taken such that both U^{rw} and its derivative vanish at $z = \sigma/2$. This was the form of the interaction potential used in our previous simulations on good solvent brushes, and it ensures that no monomer can cross the grafting surface. However, after completing a detailed study using this potential, we decided it would also be of interest to include the effect of surface attraction between the polymer monomers and the wall.[2,7,16,45,46] Therefore, in some additional runs, we replaced the purely repulsive wall–monomer interaction with a long-range attractive interaction of the form

$$U^{aw} = 4\pi\bar{\rho}\epsilon^{aw}\left[\frac{1}{5}\left(\frac{\sigma}{z-\sigma/2}\right)^{10} - \frac{1}{2}\left(\frac{\sigma}{z-\sigma/2}\right)^{4}\right] \tag{6}$$

where ϵ^{aw} is the interaction strength. This form of the interaction arises from assuming a Lennard-Jones interaction between the monomers and the surface atoms and integrating over the xy plane. In the present simulations, we took the density of surface atoms $\bar{\rho} = 0.80$ and varied ϵ^{aw}. In most of the runs we used only the repulsive wall potential U^{rw}, except when we explicitly studied the effect of the attractive interaction on the monomer density profile in section III. In this case we turned off the repulsive wall–monomer potential and let $\epsilon^{aw} \neq 0$. However, for small ϵ^{aw} ($\sim 0.1\epsilon$), the repulsive part of U^{aw} dominated, and the results were the same for both potentials. Results for the attractive potential agree better with recent neutron reflectivity experiments by Perahia *et al.*[44] of polystyrene end grafted onto silicon which show a small surface excess.

The equations of motion[47] of the monomers are integrated using a velocity-Verlet algorithm with a time step Δt, taken to be as large as possible, while keeping the integration stable. We used $\Delta t = 0.012\tau$ for the athermal case and $(0.006–0.008)\tau$ for T in the vicinity of T_θ, where $\tau = \sigma(m/\epsilon)^{1/2}$. The friction coefficient Γ was set to be $\Gamma = 0.5\tau^{-1}$. We used units in which $m = \sigma = 1$ and measured the temperature in units of ϵ/k_B. Further details on the simulation technique can be found elsewhere.[48]

Using this method, we simulated brushes consisting of $N + 1$ monomers, with $N = 50$, 100, and 200 at the following surface densities ρ_a: 0.03, 0.07, and 0.1 in units of σ^{-2}. The first monomer of each chain is firmly attached to the grafting surface, which is located on the xy plane. Periodic boundary conditions are used in the x and y directions. For all cases, $M = 50$ chains were attached to the surface, which is large enough so that the chains do not cross the periodic boundaries more than once.

After a long equilibration run (typically 5×10^4–10^5 time steps), the monomer coordinates were saved every 1000 time steps. Several quantities were later calculated from these configurations, including the local monomer density $\rho(z)$, the density of the free ends of the chains $\rho_E(z)$, and some measures of the brush height. The average monomer height $\langle z\rangle$ is defined as

$$\langle z\rangle = \int_0^\infty z\rho(z)\,dz \Big/ \int_0^\infty \rho(z)\,dz \tag{7}$$

The mean square end-to-end distance of the chains

$$\langle R^2\rangle = \langle(\vec{r}_{i,0} - \vec{r}_{i,N})^2\rangle \tag{8}$$

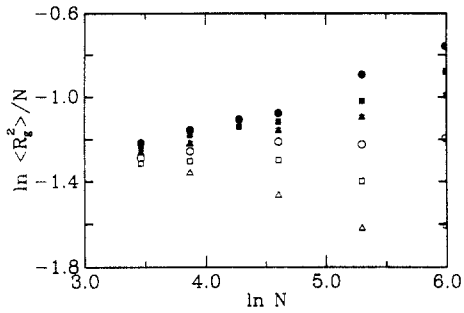

Figure 2. Mean square radius of gyration $\langle R_G^2\rangle/N$ versus N for free chains of length N = 32–400 for temperature T = 2.6 (△), 2.8 (□), 3.0 (○), 3.2 (▲), 3.4 (■), and 3.6 (●) for $r_c = 2.5\sigma$. Results indicate that $T_\Theta = 3.0 \pm 0.1$.

Table I. Properties of Polymer Brushes in a Good Solvent[a]

N	ρ_a	T_t/τ	$\langle R_G^2\rangle$	$\langle R_{Gz}^2\rangle$	$\langle R^2\rangle$	$\langle R_z^2\rangle$	$\langle z\rangle$
50	0.03	4200	26.8	15.1	230.7	159.4	7.6
50	0.07	9600	33.5	23.8	311.0	248.5	9.1
50	0.10	3000	39.3	31.2	385.3	334.6	10.5
100	0.03	3600	77.0	53.2	697.3	554.6	13.9
100	0.07	4800	112.7	94.7	1102.6	1002.0	18.1
100	0.10	6000	137.3	120.2	1384.2	1274.3	20.1
200	0.03	9600	238.0	187.4	2258.5	1954.5	25.6
200	0.07	12000	413.1	375.7	4167.8	3937.7	35.3
200	0.10	4800	528.0	497.8	5404.7	5214.6	40.2

[a] Monomer interaction with a purely repulsive potential [$r_c = 2^{1/6}\sigma$ in eq 3]. N is the chain length, T_t is the total duration of the run after equilibration, $\langle R_G^2\rangle$ is the mean square radius of gyration of the chains, $\langle R_{Gz}^2\rangle$ is the sum of the contributions to R_G^2 in the direction perpendicular to the surface, $\langle R^2\rangle$ is the mean square end-to-end distance, $\langle R_z^2\rangle$ is the sum of the contributions to R^2 in the direction perpendicular to the surface, and $\langle z\rangle$ is the average monomer height. All simulations were run with M = 50 chains at T = 1.2.

and the mean square radius of gyration of the chains

$$\langle R_G^2\rangle = (1/N)\langle \sum_{j=1}^{N} (\vec{r}_{i,j} - \vec{r}_{i,CM})^2 \rangle \qquad (9)$$

were also calculated. Here $\vec{r}_{i,j}$ and $\vec{r}_{i,CM}$ are the coordinates of the monomer j and of the center of mass of chain i, respectively. The average enclosed in angular brackets is both an average over the M chains as well as over time (configurations). The z contributions to $\langle R_G^2\rangle$ and $\langle R^2\rangle$, denoted by $\langle R_{Gz}^2\rangle$ and $\langle R_z^2\rangle$, respectively, were also calculated.

We also evaluated the static structure factor $S(q)$ which is given by

$$S(q) = (1/NM)\langle \sum_{ij} \exp(i\vec{q}\cdot(\vec{r}_i - \vec{r}_j)) \rangle \qquad (10)$$

where the sum is over all monomers in the system. Here we choose $q = q_z$, perpendicular to the grafting plane. $S(q_z)$ is the Fourier transform of the monomer density $\rho(z)$.

III. Results

Evaluation of the Θ Temperature. The Θ temperature, T_Θ, of our model was found by simulating dilute, free chains. For a single chain, the mean square radius of gyration $\langle R_G^2\rangle \propto N^\nu$, where $\nu = 0.59$ for good solvent, 1/2 for a Θ solvent, and 1/3 for a poor solvent. Figure 2 shows our results for $\langle R_G^2\rangle/N$ versus N for chains of length 32 to 400. The data represent averages of long runs of between 5×10^6 and 25×10^6 time steps. The data clearly show that $T_\Theta = 3.0 \pm 0.1$, which is the temperature where $\langle R_G^2\rangle/N$ is independent of N for large N. For a similar model with identical interactions between monomers but a slightly different interaction between the bonded monomers Weinhold and Kumar[42] also found that T_Θ is approximately 3.0 from measurements of $\langle R_G^2\rangle/N$. However, from the chain length dependence of the incremental chemical potential, Kumar[49] found a slightly lower value for $T_\Theta = 2.75$. However, due to the uncertainties in the incremental chemical potential, this value is probably not as reliable as that determined from $\langle R_G^2\rangle/N$.[42] Baumgärtner[50] also studied a similar model; however, he did not truncate the Lennard-Jones interaction and fixed the bonded monomer distance to be $2^{1/6}\sigma$. Not surprisingly, he found a larger value for $T_\Theta = 3.7$.

In the rest of the paper, we take $T_\Theta = 3.0$.

Brush Height. In our study, we simulated a large number of brushes, with different chain lengths at several grafting densities, and at various T. A list of these cases is given in Tables I and II, along with the duration of the simulation T_t (after the brushes were equilibrated) and results for several quantities of interest, as defined in the previous section. In order to compare our results with existing theories of brushes, it was necessary that the chains strongly overlap; i.e., $\rho_a \gg \rho_a^*$, where ρ_a^* is the overlap threshold. ρ_a^* depends on N and T and scales as $\sim N^{-6/5}$

Table II. Properties of Polymer Brushes as a Function of Temperature[a]

N	ρ_a	T_t/τ	T	$\langle R_G^2\rangle$	$\langle R_{Gz}^2\rangle$	$\langle R^2\rangle$	$\langle R_z^2\rangle$	$\langle z\rangle$
50	0.03	3600	4.0	18.2	7.7	146.3	82.4	5.8
50	0.03	1800	3.0	15.8	5.5	121.6	58.5	5.1
50	0.03	1800	2.0	12.0	3.2	87.7	33.0	4.2
50	0.10	500	8.0	27.6	19.9	259.3	213.4	8.6
50	0.10	1800	4.0	23.2	14.4	207.7	154.1	7.6
50	0.10	2100	3.0	19.6	10.5	169.0	113.7	6.7
50	0.10	2400	2.0	14.1	5.0	110.1	53.6	5.1
100	0.03	1280	8.0	56.1	33.6	486.3	352.4	11.3
100	0.03	1200	4.0	42.3	22.5	349.0	235.6	9.6
100	0.03	1400	3.0	33.0	12.9	251.9	136.4	7.7
100	0.03	1600	2.0	25.4	6.2	188.5	62.2	5.8
100	0.07	1600	4.0	57.3	38.3	514.4	401.4	12.3
100	0.07	2800	3.0	42.5	24.4	356.0	356.8	10.2
100	0.07	1600	2.0	28.4	9.3	202.1	95.4	7.0
100	0.10	1000	8.0	92.4	76.4	910.4	811.1	16.4
100	0.10	1200	4.0	71.3	53.2	677.3	565.0	14.2
100	0.10	1400	3.0	56.1	36.4	508.6	387.2	12.2
100	0.10	800	2.0	35.6	16.2	279.8	165.0	8.9
200	0.03	2400	4.0	112.0	68.9	970.5	720.1	16.6
200	0.03	1050	3.0	77.9	35.8	635.1	396.8	12.8
200	0.03	800	2.0	53.3	12.0	394.8	135.2	8.6
200	0.07	1400	3.0	121.7	88.4	1107.2	915.9	18.5
200	0.10	1500	4.0	237.0	206.2	2343.2	2153.4	27.0
200	0.10	1050	3.0	174.9	139.0	1694.2	1473.0	23.1
200	0.10	800	2.0	102.1	66.5	892.2	675.8	16.6

[a] Parameters are the same as in Table I, except the range of interaction in eq 3 has been extended to $r_c = 2.5\sigma$.

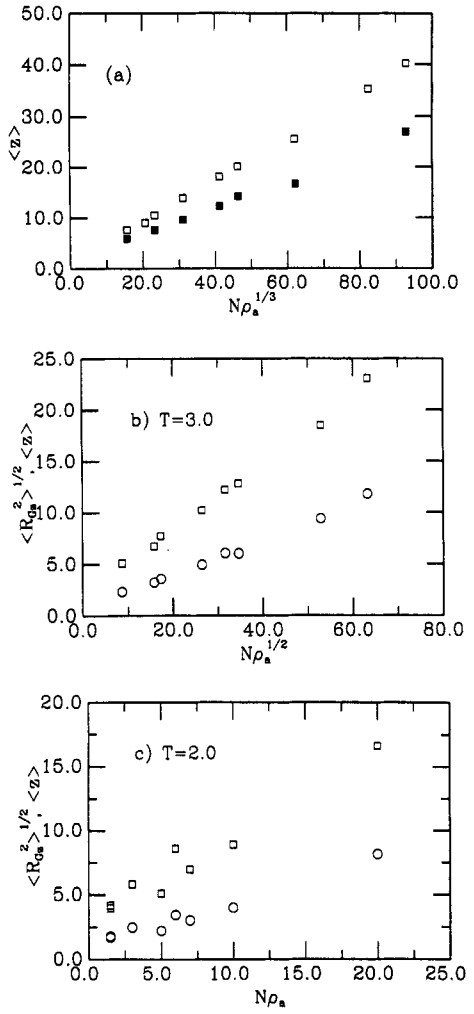

Figure 3. (a) Average monomer height $\langle z \rangle$ versus $N\rho_a^{1/3}$ for brushes in a good solvent for the athermal case $r_c = 2^{1/6}\sigma$ (□) at $T = 1.2$ and for the case with an attractive potential, eq 3 with $r_c = 2.5\sigma$ at $T = 4.0$ (■). (b) $\langle z \rangle$ (□) and the z contribution to the mean square radius of gyration $\langle R_{Gz}^2 \rangle^{1/2}$ (○) versus $N\rho_a^{1/2}$ for $T = T_\Theta = 3.0$. (c) $\langle z \rangle$ and $\langle R_{Gz}^2 \rangle^{1/2}$ versus $N\rho_a$ for $T = 2.0$.

for a good solvent, $\sim N^{-1}$ for a Θ solvent, and $\sim N^{-2/3}$ for a poor solvent. Note that, as the solvent quality decreases, ρ_a^* increases for fixed chain length. Therefore, in order to study this strongly overlapping regime, all of the simulations were carried out for $N \geq 50$ and $\rho_a \geq 0.03$. As seen from the scaling plots for the brush height h and the monomer density profiles, most of our results except for some at $\rho_a = 0.03$ satisfy this condition.

Figure 3 shows the variation of the brush height (as measured by $\langle z \rangle$ and $\langle R_{Gz}^2 \rangle^{1/2}$) as a function of the appropriate SCF scaling variable. For good solvent conditions, both for the athermal model ($r_c = 2^{1/6}\sigma$) and for $T = 4$ ($>T_\Theta$) for the longer range model with $r_c = 2.5\sigma$, the scaling variable is $N\rho_a^{1/3}$, as seen in Figure 3a. Both the scaling[2,3] and the SCF[10,38] analyses predict that the height grows linearly with this scaling variable. SCF predicts that, in the limit of strong overlap, h scales as $N\rho_a^{1/2}$ for $T = T_\Theta$ and as $N\rho_a$ for $T < T_\Theta$. As can be seen in Figure 3a,b, this scaling holds very well for all brushes studied for T at and above the Θ temperature, indicating that, for the surface coverages and chain lengths considered here, the chains are strongly overlapping. The dependence on the appropriate scaling variable is linear, considering that the calculated heights have an uncertainty of about 5% (this estimate is based upon the height values from averaging over half the simulation time). For $T = 2$ ($\ll T_\Theta$), however, the agreement with the SCF prediction is very poor. Although there is a roughly linear increase of height with $N\rho_a$, the dependence is rather erratic, and does not even seem to be monotonic. However, as will be shown below, some of our systems, particularly those that are not strongly overlapping, exhibit a strong phase separation below T_Θ when the surface density is below 0.1 for the chain lengths studied here.

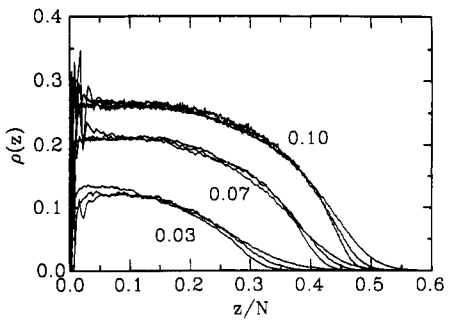

Figure 4. Monomer number density, $\rho(z)$, as a function of the distance from the grafting surface for chains of length $N = 50$, 100, and 200 for $\rho_a = 0.03$, 0.07, and 0.10 for brushes in a good solvent (athermal case).

As we will show in the following sections, the actual monomer density within the brush for T near and below T_Θ violates the condition that the average density remain low, which is required for the applicability of the simple SCF analysis which includes only binary interactions.[36,38] This violation will be shown to lead to deviations from the SCF predictions of the density profile even at $T \simeq T_\Theta$. The results for the brush height show that even though the monomer densities do not seem to be high enough to affect the *scaling* of the height at T_Θ, they are sufficiently high that they alter the scaling of the density profiles for lower T.

IV. Structure of the Brush

Good Solvent Conditions. The structure of brushes under good solvent conditions was studied in detail in a previous publication.[14] In the present study, we report additional simulations using longer chains for the athermal case with $r_c = 2^{1/6}\sigma$. We also calculate the structure factor of our brushes, allowing for a comparison with scattering experiments. Mapping of our simulations to experiments on end-functionalized polystyrene in good solvent is discussed in the Appendix.

Figure 4 shows the monomer density as a function of the distance from the grafting surface (scaled by the chain length) for brushes at a grafting density of $\rho_a = 0.03$, 0.07, and 0.10. The profiles overlap at all values of z/N for the larger two coverages, except at the free ends of the brush, where the density decays gradually instead of at a well-defined value of z/N. This foot is an exponential decay of the segment density profile, caused by fluctuations of the average trajectory of the chains near the ends where the chain stretching is weak.[8] The SCF prediction for the monomer density profile at good solvent conditions can be written as $\rho(z) = C_1\rho_1^{2/3} - C_2(z/N)^2$, where C_1 and C_2 are constants independent of ρ_a and N. The fact that these profiles overlap when plotted as a function of z/N demonstrates the validity of the SCF analysis for the good solvent conditions. Further demonstrations of its validity were presented in ref 14, in which C_1 and C_2 were explicitly calculated from a parabolic fit and were shown indeed to be independent of N and ρ_a. Lai and Zhulina[51] have also carried out detailed comparisons between the SCF theory and Monte Carlo simulations using the bond fluctuation model. At high surface coverages,[14,18,52] it is important to note that the profiles become flatter than a parabola, in agreement with Shim and Cates.[12]

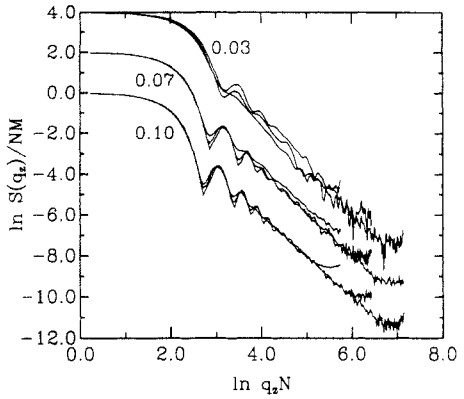

Figure 5. Scaling plot of the static structure function $S(q_z)/NM$ versus q_zN for brushes in a good solvent. Results for 0.03 and 0.07 are shifted vertically for clarity.

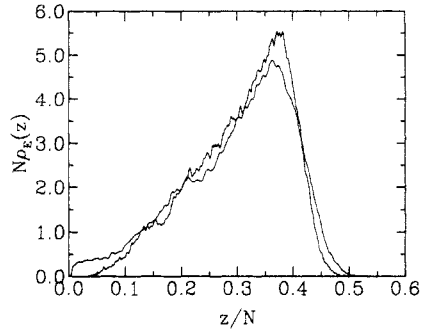

Figure 6. Scaled probability of finding a free end of a chain at a distance z from the grafting surface, $\rho_E(z)$, versus z/N for coverage $\rho_a = 0.07$ and $N = 100$ and 200 in a good solvent.

Though not shown clearly in Figure 4, there is a small depletion zone of about 4σ near the surface where the monomer density is reduced from its maximum value in agreement with earlier Monte Carlo simulations by Chakrabarti and Toral.[15] While the relative size of this regions shrinks as N increases,[9] it may be important in fitting profiles for short and intermediate chain lengths. As shown below the size of the depletion zone increases as T decreases.

In Figure 5 we present scaling results for the static structure factor $S(q_z)$ versus q_zN for all three coverages under good solvent conditions. Here q_z is the scattering vector perpendicular to the grafting plane. Note that there is very good overlap for the larger two coverages. However, for lower coverage $\rho_a = 0.03$, we observe deviations from the SCF scaling similar to that observed in $\rho(z)$. The deviations result from the fact that, at low surface coverage, the individual chains do not overlap sufficiently (especially for the smaller N) and as a result do not stretch enough, violating one assumption of the SCF. For $\rho_a = 0.03$, much longer chains would be necessary to reach the scaling regime.

The density of the free ends, $\rho_E(z)$, for brushes at a surface coverage of 0.07 is shown in Figure 6 for chain lengths $N = 100$ and 200. The SCF prediction[10,38] for $\rho_E(z)$ is that $\rho_E(z) \propto \rho_a^{-2/3}N^{-1}(z/N)f(z/N\rho_a^{1/3})$, with different functional forms of f at moderate- and high-density regimes. Thus, for a given surface density, plots of $N\rho_E$ versus z/N for different brushes should overlap. The behavior shown in Figure 6 is clearly in accordance with this prediction. Further tests of agreement of $\rho_E(z)$ with the SCF analysis for good solvent conditions can be found in refs 14 and 51.

A recent experimental study,[34] in which the polymer–polymer structure factor was directly measured, has confirmed that the density profile can be described by a parabolic shape, with a small exponential tail. On the basis of this and a variety of earlier simulation results,[14-18] one can conclude that SCF gives an adequate description of brushes at good solvent conditions.

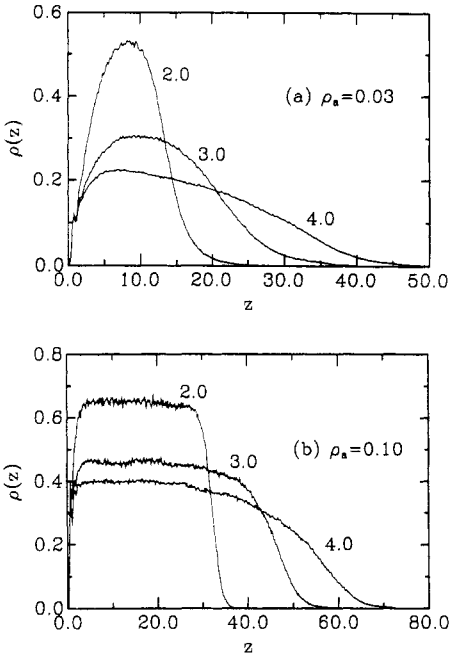

Figure 7. Monomer number density $\rho(z)$ versus z for chains of length $N = 200$ at $T = 2.0$, 3.0, and 4.0 for (a) $\rho_a = 0.03$ and (b) $\rho_a = 0.10$.

Now we consider brushes in which the attractive interaction between the monomers is included by extending the range of the Lennard-Jones potential to $r_c = 2.5\sigma$. Simulations for $T = 4.0$ ($>T_\Theta$) gave results similar to those presented above (see Figure 3a) for the good solvent case and will not be discussed in detail.

Θ Temperature Conditions. Figure 7 shows the variation of the density profiles of the brushes for $N = 200$ at two different surface coverages for several values of T. The brush height decreases considerably with decreasing T, with a corresponding increase in the average monomer density within the brush. For $\rho_a = 0.1$, the profile is almost a step function, except for a small exclusion zone near the grafting surface.

The SCF prediction for the density profile near the Θ temperature is[38]

$$\rho(z) = C_3\rho_a^{1/2}[1 - C_4(z/N\rho_a^{1/2})^2]^{1/2} \qquad (11)$$

with C_3 and C_4 independent of N and ρ_a. To test this prediction, we show in Figure 8 $\rho(z)$ for $N = 200$ together with the functional form given by eq 11, with C_1 and C_2 chosen to give the best fit to the profiles subject to the normalization constant that the area under each curve is $N\rho_a$. As one can easily see, the fit is not satisfactory. Part of the difficulty is that, as one approaches T_Θ, the monomers prefer to be near each other instead of the solvent. This results in a relatively large monomer density on the order of 0.4–0.45 as seen in Figure 8 and a flatter profile than predicted by eq 11.[38] These large values of the density are about half of those for a polymer melt for this model[53] and are large enough that one should not expect the simple SCF theory with only binary interactions to be applicable. One possibility of having strongly overlapping chains, $\rho_a \gg \rho_a^* \approx N^{-1}$, and yet keeping the overall monomer density less than about 0.2 is to increase N and reduce the surface coverage ρ_a. However, as seen in Figure 9 for $\rho_a = 0.03$, this does not really help, at least for our model, since as N increases, the maximum value of the density also increases. For our longest chains (N

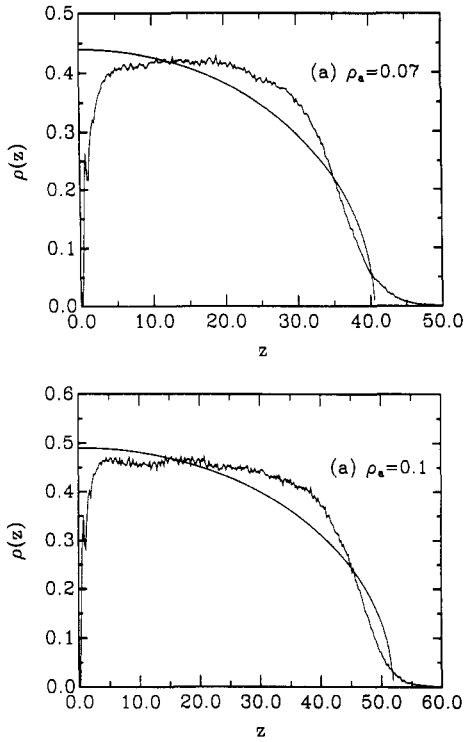

Figure 8. Monomer number density $\rho(z)$ versus z for chains of length $N = 200$ at $T = T_\Theta$ for (a) $\rho_a = 0.07$ and (b) $\rho_a = 0.10$. The smooth curve is the form predicted by the SCF, $(1 - \beta z^2)^{1/2}$, normalized so that the areas under the curves are identical.

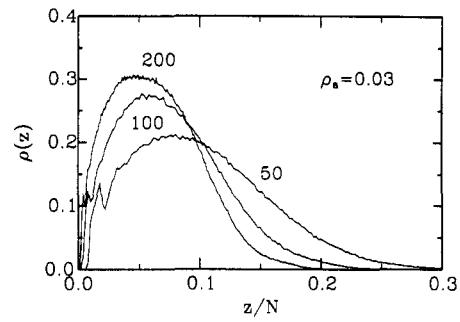

Figure 9. Monomer number density $\rho(z)$ versus z for chains of length $N = 50$, 100, and 200 at $T = T_\Theta$ for $\rho_a = 0.07$.

= 200), the density has not even reached saturation, indicating that even reducing the coverage may not be sufficient to satisfy the condition that binary interactions dominate which was of the SCF theory. The results shown in Figure 9 are however in qualitative agreement with the SCF calculations of Whitmore and Noolandi[37] for finite chain lengths. They find that, for degrees of polymerization appropriate for many experimental systems, $\rho(z)$ does not scale with z/N.

Lai and Binder[41] also found significant deviations of the density profile at T_Θ from the form given by the SCF analysis. However, their monomer density profiles, when scaled by $\rho_a^{1/2}$, collapsed into a single (albeit thick) curve when plotted as a function $N\rho_a^{1/2}$. This is not in accordance with our conclusion based on data such as those shown in Figure 9. A careful look into their results reveals that this collapse is for only two chain lengths (30 and 40 or 40 and 50) for a given ρ_a. We predict that their scaling plot would not be as good if a wider range of chain lengths were used, as was done here. A quantity related to the density profile is the structure factor which is shown in Figure 10 for $\rho_a = 0.07$ and 0.10 for $T = T_\Theta$. Similarly to the density profiles, the data do not collapse.

Comparing the density of the free ends for $\rho_a = 0.07$ and $N = 100$ and 200 at T_Θ shown in Figure 11 with the same

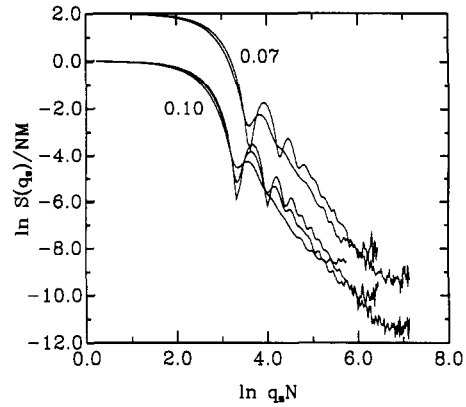

Figure 10. Scaling plot of $S(q_z)/NM$ versus q_zN for brushes at $T = T_\Theta$ for two coverages. Results for 0.07 are shifted vertically for clarity.

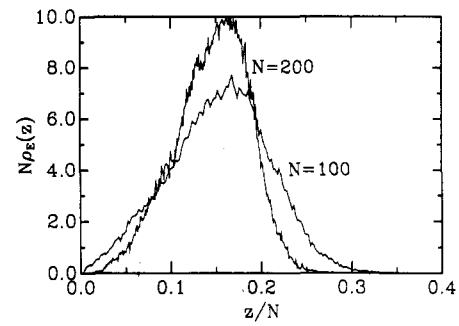

Figure 11. $N\rho_E(z)$ versus z/N for coverage $\rho_a = 0.07$ and $N = 100$ and 200 at $T = T_\Theta$.

quantity at good solvent conditions (see Figure 6), we find that the qualitative picture is similar. To compare the functional form of $\rho_E(z)$ with the SCF predictions, we note that the latter predicts $\rho_E(z) \simeq (1/N\rho_a^{1/2})f(z/N\rho_a^{1/2})$, up to the brush height, at which point it drops sharply to zero. Although a roughly linear increase is visible for small z, there is no evidence of a sharp cutoff at large values of z for the chain lengths studied. Not surprisingly, our results for $N\rho_a^{1/2}\rho_E(z)$ do not collapse onto a single scaling curve. Lai and Binder[41] have also looked at the scaling plots of $\rho_E(z)$ at the Θ conditions. They concluded that the data for several (N, ρ_a) pairs collapse, although the functional form predicted by SCF is not observed. However, their scaling plot is again rather thick, especially near the maximum of $\rho_E(z)$, even though the range of surface densities covered in their study is rather small ($0.075 < \rho_a < 0.125$). We again predict that the data collapse will become much worse when a larger range of ρ_a is considered.

Poor Solvent Conditions. For T much below T_Θ, the density profile of the brush becomes steplike and relaxation becomes slow. To check that our results in this low T regime were equilibrated, we carried out several additional simulations. Most of our data for $T = 2.0$ were obtained by cooling from $T = 3.0$. However, in some runs, we first compressed the brush at high temperature, $T = 4.0$, with a purely repulsive plate parallel to the grafting plane. After compressing the upper plate so that the brush height was the same as that of the brush obtained by cooling from $T = 3.0$, we cooled the system to $T = 2.0$. We then removed the upper plate and let the system run an additional 500τ. Results for both cases were the same within statistical error.

Figure 12 shows $\rho(z)$ for $\rho_a = 0.10$ at $T = 2$. The highest concentration obtained seems to be around 0.67, close to melt densities for this model.[53] For lower coverages, where ρ_a is near the overlap threshold ρ_a^*, we observe strong phase separation where the surface is partially exposed in

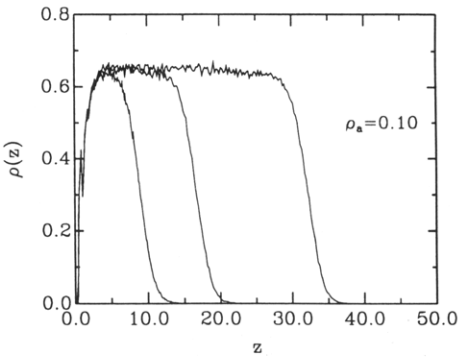

Figure 12. Monomer number density $\rho(z)$ versus z for chains of length N = 50, 100, and 200 at T = 2.0 for ρ_a = 0.10.

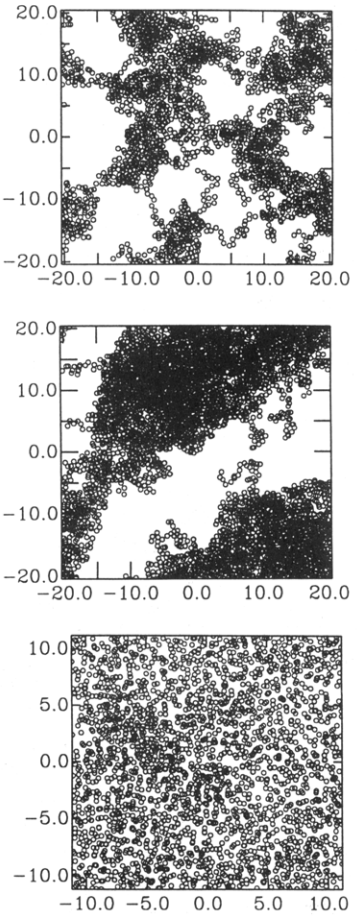

Figure 13. Projection of all monomers onto the z = 0 plane below T_Θ at T = 2.0 for (a, top) N = 50 and ρ_a = 0.03, (b, middle) N = 100 and ρ_a = 0.03, and (c, bottom) N = 50 and ρ_a = 0.10 for ends randomly grafted.

agreement with Lai and Binder.[41] When the chain length or the grafting density increased, the holes gradually disappeared. We find, for instance, that for ρ_a = 0.03 the projection on the xy plane of all the monomers at T = 2 for N = 50 shows a phase separation with several regions free of monomers (Figure 13a). When one looks at brushes with N = 100 (Figure 13b; a three-dimensional picture of this snapshot was shown in Figure 1), there is a single hole whose size diminishes with increasing N. Even for N = 200, this hole remains. For longer chain lengths, we expect that the surface will not be exposed but that the density profile may not be uniform.[40] For larger coverages, like ρ_a = 0.1, even brushes of chain length N = 50 do not exhibit the strong phase separation (Figure 13c) observed for ρ_a = 0.03; However, we are unable to say if the surface is "uniform" or "dimpled". Yeung *et al.*[40] predict that a transition from a dimpled surface to a uniform one appears

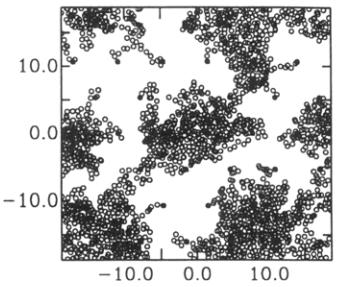

Figure 14. Projection of all monomers onto the z = 0 plane below T_Θ at T = 2.0 for N = 50 and ρ_a = 0.03 for a triangular lattice array of grafting points.

at larger values of N for lower surface coverages in agreement with our results.

We also observed the formation of holes when the grafting sites were placed on a lattice. Figure 14 shows a snapshot of the simulation, with all the monomers projected onto the xy plane for N = 50 and ρ_a = 0.03. The grafting sites (shown as large full dots) are on a triangular lattice plane. Note that the monomers are clustered in several regions arranged in a triangular array. Therefore, the phase separation is not due solely to the random placement of the grafting sites.

V. Attractive Surface–Monomer Interaction

All of the results discussed so far have been for a purely repulsive wall–monomer interaction. For all temperatures studied, this repulsive interaction gave rise to a small exclusion zones near the grafting surface, where the monomer density is lower than that of the bulk. As T is reduced, the monomers reduce their free energy by being next to each other rather than the repulsive wall and this region becomes more pronounced as seen from Figure 7. The size of the region is independent of N as seen in Figure 12. However, in many experimental situations it is possible that the surface will have at least a weak attractive interaction with the monomers of the chain. Therefore, to study the competition between the attraction each monomer has for another monomer and for the wall, we carried out a number of runs for N = 100 for varying surface–monomer couplings using the longer range interaction given by eq 6. Previously Chakrabarti *et al.*[16] studied the effect of surface attraction for a good solvent.

Parts a and b of Figure 15 present our results for $T = T_\Theta$ for ρ_a = 0.03 and 0.07. Note the strong increase in the monomer density near the wall as ϵ^{aw} increases. For ϵ^{aw} on the order of ϵ and greater, a surface excess appears. Results for $\epsilon^{aw} = \epsilon$ for three values of T are shown in Figure 15c. While we have not carried out a detailed comparison, these results agree reasonably well with recent measurements of the monomer density profile for end-functionalized polystyrene grafted onto silicon which definitely show that there is an excess surface layer of polystyrene near the surface.[44]

VI. Summary and Outlook

We have made a detailed numerical study of the structure of end-grafted polymeric chains (brushes) at fixed coverage under good, Θ, and poor solvent conditions. For the good solvent case, we find very good agreement with the SCF predictions. The brush height, as well as the density profiles of the monomers and the free ends of the chains, scales with the chain length and the surface coverage as predicted. The same is true for the structure factor. Detailed agreement with SCF can be found in the functional forms of the density profiles as well. MC simulations by Lai and Zhulina[51] also found very good

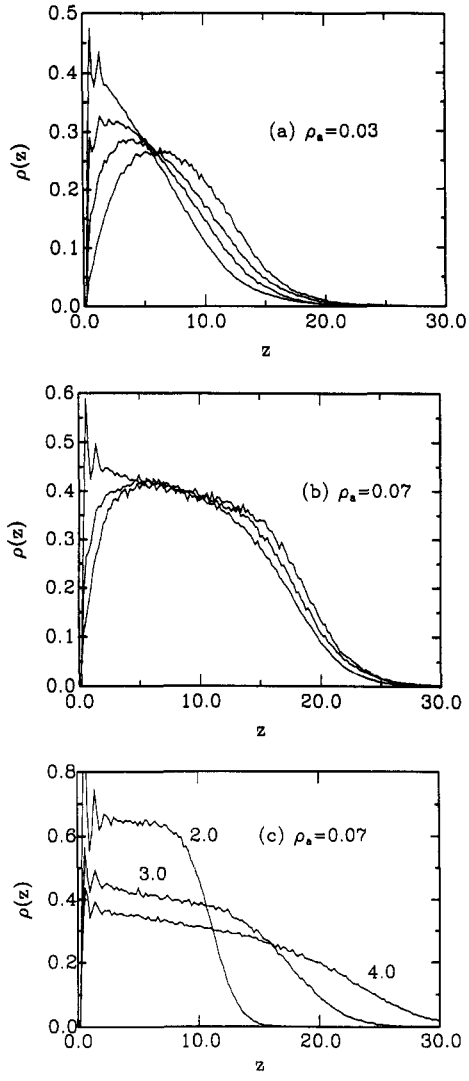

Figure 15. Monomer number density $\rho(z)$ versus z for chains of length $N = 100$ and (a) $\rho_a = 0.03$ for $\epsilon^{aw}/\epsilon = 0.1$, 0.5, 0.75, and 1.0 at $T = T_0$, (b) $\rho_a = 0.07$ for $\epsilon^{aw}/\epsilon = 0.1$, 0.5, and 1.0 at $T = T_\Theta$, and (c) $\rho_a = 0.07$ for $\epsilon^{aw} = \epsilon$ at $T = 2.0$, 3.0, and 4.0. Increasing ϵ^{aw} increases the density of monomers near the surface.

agreement. Considering the fact that a recent experimental study[34] confirmed the parabolic monomer density profile predicted by SCF, our results reiterate the conclusion that the SCF description of the brushes at good solvent conditions is very good. Mapping of our bead-spring model to experiments is discussed in the Appendix.

However, for the same systems for which SCF works well under good solvent conditions, SCF predictions do not seem to hold as well as the solvent quality is decreased. We find that, at Θ solvent conditions, the density profile cannot be described by the SCF functional form for the range of chain lengths studied here. The same is true for the density profile of the free ends and for the structure factor. Interestingly enough, however, the height of the brush does scale as $N\rho_a^{1/2}$, in agreement with the results of the SCF analysis. The reason for this lack of agreement with the SCF theory is the relatively large monomer densities for temperatures in the vicinity of T_Θ. In principle for very long chains and low surface coverages it may be possible to be in a situation in which the monomer density is small even near T_Θ although we were unable to locate such a regime. Unfortunately this regime seems to be difficult to achieve. On the basis of the mapping to experimental polymers discussed in the Appendix, we believe that our simulated chains are equivalent to most, if not all, present experimental studies on brushes, suggesting that experimentally it may also be difficult to satisfy both the strong overlap and dominance of binary interactions implicit in the analytic SCF treatment of ref 38.

At even lower temperatures (poor solvent conditions), not all of our data for h conform to the SCF scaling, which should be proportional to $N\rho_a$. This disagreement can be attributed to the fact that for some of our runs the chains are not strongly overlapping which results in a strong phase separation of the brush into monomer-rich and monomer-poor regions for low surface coverage and short chains. For higher coverages and longer chains, the scaling predictions are satisfied. Note that this phase-separated phase should only be seen for chemically absorbed chains in equilibrium with a polymer-free solution. If there are any chains in solution, then one would expect that below T_Θ these chains will phase separate to the surface, filling in the exposed surface.

Because our chains are grafted to the surface with infinite binding energy, the only effect of varying T is to change the relative interaction between the monomers. This will be the dominant effect for polymers which are chemically attached to the surface or for diblocks with long anchoring blocks. However, for brushes absorbed with lower binding strength, changing T may also change the surface coverage. For the case of polystyrene end functionalized with zwitterions, the binding energy is only on the order of $(6–8)k_BT$ and ρ_a is observed to depend significantly on the chain length ($\rho_a \approx N^{-2\nu}$). Taunton *et al.*[25] explained this dependence by noting that each k_BT of binding energy could support about one blob. The larger N, the larger each blob would be, resulting in a lower surface coverage. Similar effects are expected and have been observed[44] as T is varied. Perahia *et al.*[44] found using neutron reflectivity that, as T decreased, the surface coverage increased. Unfortunately this means that direct comparison of our simulations as well as those by Lai and Binder[41] cannot be made. At the present time it is also not possible to simulate end-grafted polymers with a finite binding energy in equilibrium with polymers in solution due to the slow equilibration of the exchange except for very short chains.[54] An alternative is to use constant-pressure simulations in which the surface coverage is allowed to vary.[55] Results using this method suggest that the brush height h should be nearly constant as T is varied in agreement with recent results of Perahia *et al.*[44] for end-functionalized polymers grafted on silicon.

Acknowledgment. We thank D. Perahia for helpful discussions.

Note Added in Proof: Huang and Balazs[56] have recently shown that when the SCF calculations are done in two-dimensions (the polymer density is assumed to depend on directions perpendicular and parallel to the surface), the polymer density profiles actually reveal qualitative agreement with the clumping in poor solvents observed here and in ref 41.

Appendix

In ref 53, Kremer and G.S.G. discussed how to map simulations on the bead-spring model for polymer melts to experimental polymeric systems. By comparing the entanglement length N_e to the entanglement molecular weight M_e and the diffusion constants for short chains, we were able to map both the length scale σ and the time scale τ for our coarse grain model to polystyrene, polyethylene, and several other experimental systems. This mapping proved to give an accurate prediction for the crossover time τ_e where the mean square displacement of a monomer crossedover from Rouse to reptation-like

Table III. Mapping of Simulation Results to Experiment[a]

ρ_a	N	s/σ	σ (Å)	R (Å)
0.03	132	5.8	14.7	321
0.07	65	3.8	22.5	323
0.10	48	3.2	26.9	323

[a] Mapping of simulation results for three surface coverages ρ_a to polystyrene of MW = 140 000 in toluene grafted onto mica. For this system h = 650 Å, s = 85 Å, and R_F = 323 Å.[25]

behavior.[53] Here we show that a similar type of mapping can be utilized in comparing the present simulations to experiment.

Experimentally, brushes are made by grafting either end-functionalized polymers or diblock copolymers onto a surface. Since our model polymers are grafted onto the surface at a single point, they correspond most closely to the end-functionalized polymers which can be absorbed either physically[25,28] or chemically.[32-34] Three experimental quantities which are needed for this mapping are the brush height h, the mean distance between grafting sites s, and the end-to-end distance of the free chain. For end-functionalized polystyrene in toluene grafted onto mica, Klein and co-workers[25] have measured these three quantities for a range of molecular weights from 26 500 to 660 000. Once this mapping is complete, we can use the simulation to predict properties of the system which are not easily accessible experimentally, like the monomer density profile and amount of interpenetration of polymers from one brush into the other as the two surfaces are compressed as in the surface force apparatus.

For a good solvent in the scaling regime, the average monomer height scales as $\langle z \rangle \propto N\rho_a^{1/3}$, as shown in Figure 3a. From the density profiles, such as those shown in Figure 4, we can also measure the brush height which can be compared directly by the surface force apparatus.[28] For the athermal model ($r_c = 2^{1/6}\sigma$), we find that $h = aN\rho_a^{1/3}$, where $a \approx 1.07$. The mean distance between grafting sites $s = \rho_a^{-1/2}$ within factors on the order of unity. The ratio $b = h/s$, which is approximately the number of blobs per chain and gives a characteristic measure of the amount each chain is stretched, is given by

$$b = h/s = a\rho_a^{5/6}N \tag{12}$$

Thus, for a given value of b, there is a unique relation between chain length and surface coverage ρ_a, namely

$$N = (b/a)\rho_a^{-5/6} \tag{13}$$

For polystyrene in toluene grafted onto mica this ratio is in the range 6–8. The remaining quantity of interest, namely, the mean square end-to-end distance of the free chain, can easily be measured in a separate simulation. There we found $\langle R^2 \rangle = cN^{2\nu}$, where $c = 1.5$ and $\nu = 0.59$. This last quantity is useful as an independent check that the mapping is consistent.

To test this mapping more explicitly, we compare our simulations to polystyrene of MW = 140 000 in toluene grafted onto mica. Taunton *et al.*[25] found that for this case h = 650 ± 50 Å, s = 85 Å, and the Flory radius for a free chain was 323 Å. Substituting $b = 7.6$ into eq 13, for the three values of ρ_a studied here, yields the corresponding values for N which are shown in Table III. Note that the results for N are in the range studied here. To determine which coverage is most appropriate, we can try to use R_F. However, for all three cases, $\langle R^2 \rangle^{1/2}$ is approximately 323 Å, nearly independent of ρ_a and equal to the experimental value for the Flory radius (the exact agreement is clearly fortuitous). The reason is that, for a fixed number of blobs $b = h/s$, the ratio h/R depends only very weakly on the coverage, $h/R \propto \rho_a^{1/3-5(1-\nu)/6} = \rho_a^{-0.0086}$ for $\nu = 0.59$. Therefore, to choose the appropriate coverage for this case, we cannot use R_F. However, from our simulations of the force between parallel plates containing end-grafted polymers,[30] coverages in the range of 0.03 agreed much better with the surface force data of Taunton *et al.*[25] than did 0.10. For a larger MW = 375 000, Taunton *et al.*[25] found h = 1200 ± 50 Å, $s \approx$ 150 Å, and R_F = 575 Å. Following the same analysis, for ρ_a = 0.03, we find N = 139 and σ = 25.9 Å. The corresponding end-to-end distance is 583 Å. Because the mean spacing between grafting sites decreases significantly as MW increases, the two molecular weights map to nearly identical values of N within experimental error. Therefore, for these end-functionalized polymers, simulations with ρ_a in the range 0.03–0.07 and N around 100 should describe the end-functionalized zwitterionic systems very well. A similar mapping can be carried out for the chemically absorbed systems by Auroy and co-workers.[34-34] However, in this case, since the ratio h/s is not constant, N for their highest surface coverages[33] turns out to be in the range of 300–500.

Experimentally the surface force apparatus measures the force between two brushes but does not give any information about the monomer density profiles, the distribution of chain ends, or amount of chain interpenetration. Using the above mapping and our earlier simulations,[30] we can determine these and other quantities. In ref 30, we found that the amount of interpenetration $I(D) = N^{2/3}h^{-4/3}f(D/2h)$, where D is the distance between the two plates and $f(x)$ is a scaling function which we plot in ref 30. $I(D)$ is defined as the relative number of monomers of one of the brushes that have penetrated into the region $z > D/2$. If we map our data for ρ_a = 0.03 and N = 132, to MW = 140 000, we find that $I(D) = 0.17f(D/2h)$. For a compression of 50%, that is, when $D = h$, $I(D) = 0.07$. Noting that the number of blobs per chain is b = 7.6, this corresponds to about half a blob. For $D = h/2$, $I(D) = 0.17$ which is about 1.3 blobs. These results change very little when data for ρ_a = 0.07 is used instead of 0.03. This result suggests that the onset of glassy relaxation under shear as seen by Klein, Perahia, and Warburg[28] occurs when the amount of interpenetration reaches about one blob, a quite reasonable result.

References and Notes

(1) Milner, S. T. *Science* **1991**, *251*, 905.
(2) Alexander, S. *J. Phys. (Paris)* **1977**, *38*, 983.
(3) de Gennes, P.-G. *Macromolecules* **1980**, *13*, 1069.
(4) Hirz, S. M.Sc. Thesis, University of Minnesota, 1987.
(5) Cosgrove, T.; Heath, T.; van Lent, B.; Leermakers, F.; Scheutjens, J. *Macromolecules* **1988**, *20*, 1692.
(6) Skvortsov, A. M.; Gorbunov, A. A.; Pavlushkov, I. V.; Zhulina, E. B.; Borisov, O. V.; Pryamitsyn, V. A. *Polym. Sci. USSR (Engl. Transl.)* **1988**, *30*, 1706.
(7) Muthukumar, M.; Ho, J.-S. *Macromolecules* **1989**, *22*, 965.
(8) Milner, S. T. *J. Chem. Soc., Faraday Trans.* **1990**, *86*, 1349.
(9) Wijmans, C. M.; Scheutjens, J. M. H. M.; Zhulina, E. B. *Macromolecules* **1992**, *25*, 2657.
(10) Milner, S. T.; Witten, T. A.; Cates, M. E. *Macromolecules* **1988**, *21*, 2610; *Europhys. Lett.* **1988**, *5*, 413.
(11) Zhulina, E. B.; Borisov, O. V.; Pryamitsyn, V. A. *J. Colloid Interface Sci.* **1990**, *137*, 495.
(12) Shim, D. F. K.; Cates, M. E. *J. Phys. (Paris)* **1989**, *50*, 3535.
(13) Lai, P.-Y.; Halperin, A. *Macromolecules* **1991**, *24*, 4981.
(14) Murat, M.; Grest, G. S. *Macromolecules* **1989**, *22*, 4054.
(15) Chakrabarti, A.; Toral, R. *Macromolecules* **1990**, *23*, 2016.
(16) Chakrabarti, A.; Nelson, P.; Toral, R. *Phys. Rev. A* **1992**, *46*, 4930.
(17) Dickman, R.; Hong, D. C. *J. Chem. Phys.* **1991**, *95*, 4650.
(18) Lai, P.-Y.; Binder, K. *J. Chem. Phys.* **1991**, *95*, 9288.
(19) Carignano, M. A.; Szleifer, I. *J. Chem. Phys.* **1993**, *98*, 5006.
(20) Milner, S. T.; Witten, T. A. *J. Phys. (Paris)* **1989**, *49*, 1951.
(21) Ball, R. C.; Marko, J. F.; Milner, S. T.; Witten, T. A. *Macromolecules* **1991**, *24*, 693.

(22) Birshtein, T. M.; Borisov, O. V.; Zhulina, E. B.; Khokhlov, A. R.; Yurasova, T. A. *Polym. Sci. USSR (Engl. Transl.)* **1987**, *29*, 1293.
(23) Dan, N.; Tirrell, M. *Macromolecules* **1992**, *25*, 2890.
(24) Murat, M.; Grest, G. S. *Macromolecules* **1991**, *24*, 704.
(25) Taunton, J.; Toprakcioglu, C.; Fetters, J.; Klein, J. *Nature* **1988**, *332*, 712; *Macromolecules* **1990**, *23*, 571.
(26) Hadziannou, G.; Patel, S.; Granick, S.; Tirrell, M. *J. Am. Chem. Soc.* **1986**, *108*, 2869.
(27) Patel, S. S.; Tirrell, M. *Annu. Rev. Phys. Chem.* **1989**, *40*, 597.
(28) Klein, J.; Perahia, D.; Warburg, S. *Nature* **1991**, *352*, 143.
(29) Milner, S. T. *Europhys. Lett.* **1988**, *7*, 695.
(30) Murat, M.; Grest, G. S. *Phys. Rev. Lett.* **1989**, *63*, 1074; In *Computer Simulation of Polymers*; Roe, R. J., Ed.; Prentice-Hall: Englewood Cliffs, NJ, 1991; p 141.
(31) Cosgrove, T. *J. Chem. Soc., Faraday Trans.* **1990**, *86*, 1323.
(32) Auroy, P.; Auvray, L.; Leger, L. *Phys. Rev. Lett.* **1991**, *66*, 719.
(33) Auroy, P.; Auvray, L.; Leger, L. *Macromolecules* **1991**, *24*, 5158.
(34) Auroy, P.; Mir, Y.; Auvray, L. *Phys. Rev. Lett.* **1992**, *69*, 93.
(35) Field, J. B.; Toprakcioglu, C.; Ball, R. C.; Stanley, H. B.; Dai, L.; Barford, W.; Penold, J.; Smith, G.; Hamilton, W. *Macromolecules* **1992**, *25*, 434. Kent, M. S.; Lee, L.-T.; Farnoux, B.; Rondelez, F. *Macromolecules* **1992**, *25*, 6241.
(36) Halperin, A. *J. Phys. (Paris)* **1988**, *49*, 547.
(37) Whitmore, M. D.; Noolandi, J. *Macromolecules* **1990**, *23*, 3321.
(38) Zhulina, E. B.; Borisov, O. V.; Pryamitsyn, V. A.; Birshtein, T. M. *Macromolecules* **1991**, *24*, 140.
(39) Ross, R. S.; Pincus, P. *Europhys. Lett.* **1992**, *19*, 79.
(40) Yeung, C.; Balazs, A. C.; Jasnow, D. *Macromolecules* **1993**, *26*, 1914.
(41) Lai, P.-Y.; Binder, K. *J. Chem. Phys.* **1992**, *97*, 586.
(42) Weinhold, J. D.; Kumar, S. K. *J. Chem. Phys.*, in press.
(43) Auroy, P.; Auvray, L. *Macromolecules* **1992**, *25*, 4134.
(44) Perahia, D.; Weisler, D.; Satija, S. K.; Fetters, L. J.; Sinha, S. K. To be published.
(45) Cosgrove, T.; Heath, G.; Ryan, K.; van Lent, B. *Polym. Commun.* **1987**, *28*, 64.
(46) Szleifer, I.; Ben-Shaul, A.; Gelbart, W. M. *J. Phys. Chem.* **1990**, *94*, 5081.
(47) Allen, M. P.; Tildesley, D. J. *Computer Simulation of Liquids*; Clarendon Press: Oxford, 1987.
(48) Grest, G. S.; Dünweg, B.; Kremer, K. *Comput. Phys. Commun.* **1989**, *55*, 269.
(49) Kumar, S. K. *J. Chem. Phys.* **1992**, *96*, 1490.
(50) Baumgärtner, A. *J. Chem. Phys.* **1980**, *72*, 871.
(51) Lai, P.-Y.; Zhulina, E. B. *J. Phys. II* **1992**, *2*, 547.
(52) Milik, M.; Kolinski, A.; Skolnick, J. *J. Chem. Phys.* **1990**, *93*, 4440.
(53) Kremer, K.; Grest, G. S. *J. Chem. Phys.* **1990**, *92*, 5057; **1991**, *94*, 4103 (erratum).
(54) Lai, P.-Y. *J. Chem. Phys.* **1993**, *98*, 669.
(55) Grest, G. S. To be published.
(56) Huang, K.; Balazs, A. C. To be published. Balazs, A. C. *Acc. Chem. Res.* **1993**, *26*, 63.